Design of Mixed-mode Systems for Pulse-shape Discrimination

Bryan Orabutt*, Roger D. Chamberlain*, Jonathan Elson†, George Engel‡, Franck Delaunay§, and Lee G. Sobotka†
Email: {borabutt,roger,jmelson}@wustl.edu, gengel@siue.edu, delaunay@lpccaen.in2p3.fr, lgs@wustl.edu
*Department of Computer Science and Engineering, Washington University in St. Louis, St. Louis, Missouri, USA
†Department of Chemistry, Washington University in St. Louis, St. Louis, Missouri, USA
‡Department of Electrical and Computer Engineering, Southern Illinois University Edwardsville, Edwardsville, Illinois, USA
§LPC Caen, Normandie Université, ENSICAEN, UNICAEN, CNRS/IN2P3, Caen, France

***Abstract*—The use of a mixed-mode system for performing neutron/gamma (n/γ) pulse-shape discrimination (PSD) is investigated. Historically, PSD capable systems have been composed fully of analog electronics or use fast digitizers that allow for later analysis using digital signal processing (DSP). Analog systems are inexpensive and suitable for large detectors where hundreds, or even thousands, of detector channels are needed. However analog systems are algorithm locked. DSP-based systems allow for more complex algorithms to be used for pulse processing. If fast digitzers are required, DSP systems can be prohibitively expensive for large channel-count detectors. A topology is proposed for a PSD capable mixed-mode system that combines analog and DSP techniques. The topology is modeled in Verilog-A and analyzed using waveform data from several scintillators to show that mixed-mode systems are PSD capable and offer advantages over pure analog or DSP systems.**

I. Introduction

In nuclear science experiments it is usually necessary to determine the type of radiation, its energy and direction with considerable accuracy. Position determination often requires detector arrays with many (even thousands) of elements. The detection of neutrons and discriminating them from gamma rays is particularly difficult. The lack of an electromagnetic interaction for neutrons requires detectors of significant size, exacerbating the direction (i.e. interaction localization) determination. The most common class of neutron detectors are organic scintillators. The high hydrogen content enhances the probability of generating recoil protons.

The ionization generated by these recoil protons is more dense than that generated by the gamma-ray generated electrons from either the photoelectric effect or Compton scattering. Both recoiling protons and electrons generate copious amounts of excited molecular singlet (S^*) and triplet (T^*) states. The singlet states decay quickly (some 10's of ns) while the triplet states, where they do decay via their natural lifetime, would be so slow to be uncorrelatable to the nuclear event generating the radiation. ($T \rightarrow S$, is a forbidden electromagnetic transition.) The basis of n/γ discrimination lies in an enhanced probability that the higher density of ionization from the recoiling protons generates a significant probability of what is triplet annihilation, i.e. $T^*+T^* \rightarrow S+S^*$. The excited singlet can then emit a photon. These photons are delayed relative to those that result from the deexciting singlets directly produced by the incoming radiation by the time the excitation energy was sequestered in the triplet states. Techniques for analyzing the output waveform (pulse shape) from scintillators to extract the form of the impinging radiation are called pulse-shape discrimination. Pulse shape differences are modest and can be lost by poor pulse processing techniques or small energy deposition in the scintillator. Figure 1 shows two pulses from [1], one from a neutron and the other from a gamma ray, as recorded by the light generated by a common organic scintillator.

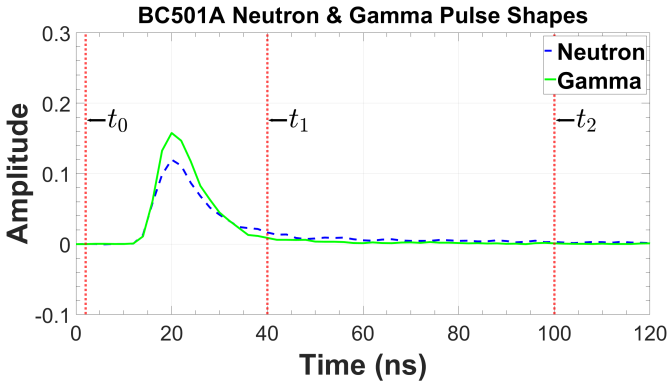

Fig. 1: n/γ waveforms from a BC501A scintillator. The time of t_2 is taken as 100 ns for illustration purposes. The real total integration gates are several hundred nanoseconds.

While there are many techniques used to quantify the difference in pulse shape, the most common is the charge comparison method (CCM). In this method, a detector pulse is integrated over two regions: the entirety of the pulse and, for example, a region in the tail of the pulse. This dual integration allows for a discriminating variable, D, to be defined

$$D = \frac{\int_{t_1}^{t_2} Q dt}{\int_{t_0}^{t_2} Q dt} \tag{1}$$

where the time range t_0 to t_2 covers the entirety of the pulse and the range t_1 to t_2 covers the pulse tail. This discriminating variable can be plotted for multiple events with respect to the

pulse energy as shown in Figure 2. This produces a bimodal distribution where the neutrons are separated from the γ-rays and a clear discrimination curve (red line) can be drawn.

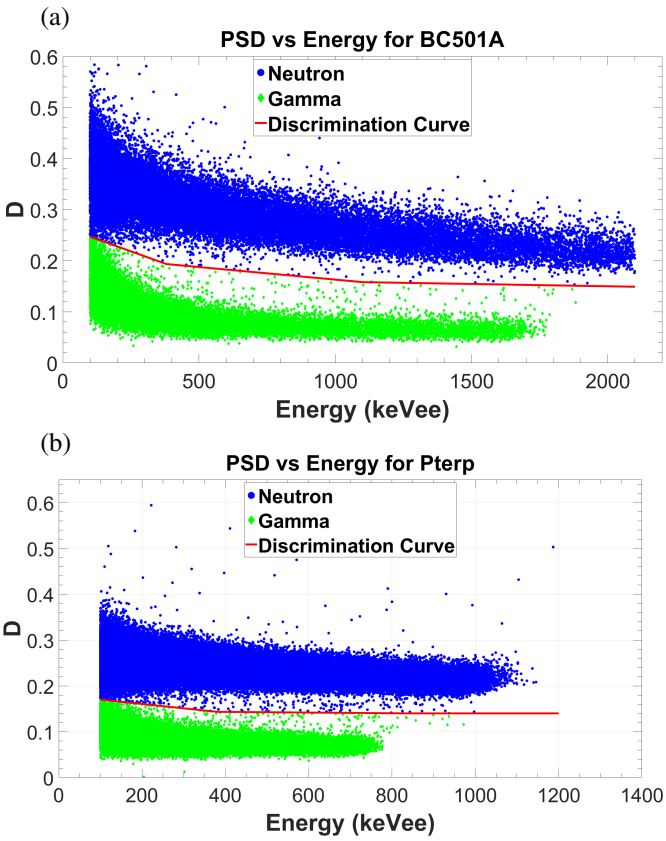

Fig. 2: n/γ discrimination in BC501A (a) and p-terphenyl (b). The units keVee are keV-electron-equivalent which describes the light output of the scinitllator with respect to the light output of an electron at a given energy. This gives a common comparison unit since electrons (gamma) and neutrons will give different light outputs for the same energy deposited.

This technique can be performed in both analog and DSP systems. In a DSP system the integrals are inferred from a summation of sample points. In an analog system multiple hardware integrators are used with different time gates to produce the two integrals. While the performance of DSP-based PSD systems is in principle superior [2], fast scintillators require fast digitizers [3], and these can be cost prohibitive for large detector arrays. In contrast, analog systems capable of PSD have been implemented on high-density integrated circuits [4], [5], making them suitable for large detector arrays. The present work investigates a system that offers the algorithm flexibility of DSP systems but, since it is an analog system, can make use of high-density CMOS circuits and thus is suitable for very large channel-count detector systems.

II. System Architecture

Figure 3 shows the proposed system. In each detector channel an integrator is sampled at fixed intervals and stored on sample and hold units (S&H). The purpose for storing these integrals rather than digitizing the integrator directly is to allow for slower, inexpensive digitizers. Each detector channel is separated into a high-gain and low-gain sub-channel for dynamic range enhancement. A small chain of sample and hold units (short buffer) is contained in each sub-channel and is used exclusively by that sub-channel. When a channel is triggered (via an external trigger circuit), the short buffer contents are retained and the channel begins sampling into one of a set of long tail buffers. The long tail buffers are global resources that can be used by any detector channel.

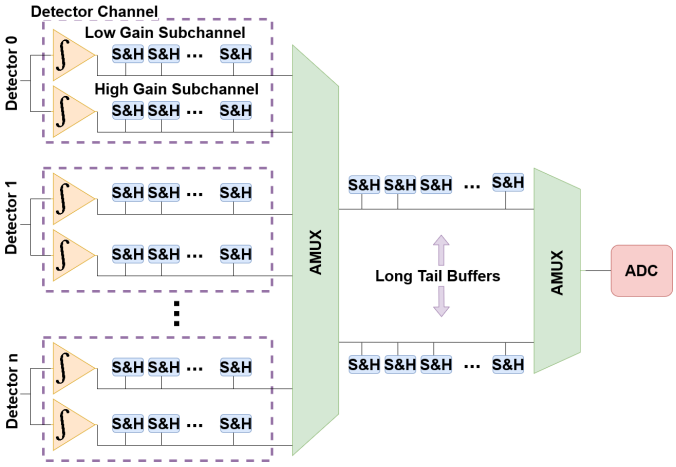

Fig. 3: Block diagram of proposed mixed-mode system.

A. Channel Specific Hardware

At the input to each sub-channel there are two programmable integrator circuits as shown in Figure 4. The two integrators are used as a ping-pong integration circuit that allows one integrator to be active while the other is being reset and vice versa. This reduces dead-time between samples which is necessary for getting adequate pulse shape information for PSD. The integrating capacitor takes 6 ns to reset which sets the lower limit on the integration period that can be used. The integrators have a programmable resistor that allows for the charge time constant to be tailored to the rise time constant of the input pulse [5].

Following each integrator is a short buffer of sample and hold units. On the rising edge of every sample clock the integral from the previous sample period is stored in the short buffer. The short buffer acts as an analog ring buffer which allows the circuit to continuously sample the detector. This ensures that no pulse information is lost and allows a baseline reading to be obtained from samples that come prior to the trigger. When radiation strikes a detector creating a pulse waveform, an off-chip constant fraction discriminator (CFD) circuit is used to indicate the onset of radiation. Such a circuit provides an amplitude-independent time reference [6] that can be used to determine the phase of the pulse with respect to the sample clock. From the CFD trigger time the peak time of the pulse can be inferred which is necessary to find the optimal

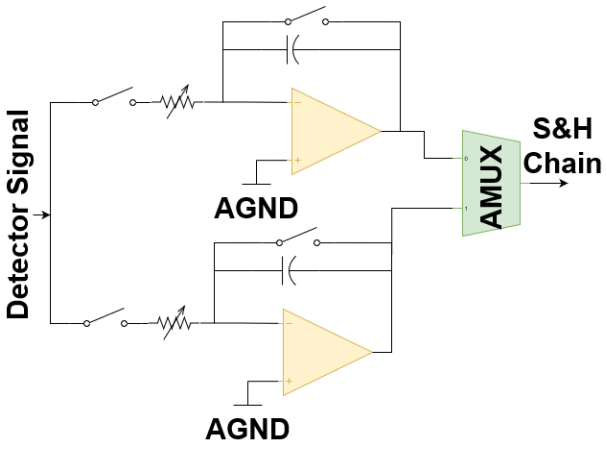

Fig. 4: Dual integrator ping-pong circuit.

late integration gate. This CFD circuit also acts as a trigger that tells the system to transition from sampling into the short buffer in the detector channel and begin sampling into one of the long tail buffers.

B. Shared Hardware

After a CFD trigger indicates pulse data is available in the short buffer, an additional k samples will be saved into the short buffer, where k is determined by the scintillator's optimal slow integration gate [1]. Once these k samples are saved, the system begins sampling into an available long tail buffer. There are fewer long tail buffers than there are detector channels, so these act as shared hardware resources. Since it is unlikely that every single channel will be hit with radiation before a full chain of short and long buffers can be digitized, it makes sense to allocate these larger buffers as shared resources to maximize the number of detector channels integrated onto one chip.

Another aspect of the long tail buffer is that it has a longer sample period than the short buffers. This is because the tail of the pulse extends much further in time than the leading edge of the pulse. To capture enough pulse shape information the system needs to integrate for a longer period of time. This could also be accomplished by adding more sample and hold units to the long tail buffers; however, this would increase the area usage of the tail buffers, negatively impacting the number of detector channels per chip.

III. Simulation Results

In order to verify that the system design is PSD capable, a single channel of the proposed topology was modeled in Verilog-A. A short buffer size of 8 sample and hold units and a long tail buffer size of 16 sample and hold units was chosen for the model. For the short buffer, a sample period of 10 ns was used, and 40 ns was used for the long tail buffers. These values have not been determined to be optimal but were chosen as reasonable values for capturing pulse shape information from the pulse data set. The pulse data is composed of real sampled waveforms (at 500 MSPS) from several different scintillators which were turned into analog pulses by connecting the sample points in a piece-wise linear fashion. The dataset was previously used for analyzing the PSD properties of different scintillators [1].

A. Pulse-shape Discrimination

The Verilog-A models were simulated with 160,000 pulses from a BC501A scintillator and performed PSD using CCM. For the proposed system the CCM algorithm is redefined from the traditional DSP method of summing sample points. The new algorithm works by drawing a boundary between *early integrals* and *late integrals* and defining the discriminating variable by

$$D = \frac{\sum_{i=c+k}^{7} S_i + \sum_{i=0}^{15} L_i}{\sum_{i=0}^{7} S_i + \sum_{i=0}^{15} L_i} \tag{2}$$

where c is the first sample after the CFD trigger, k indicates the number of early integral samples to take after the CFD trigger, and S_i and L_i denote samples in the short and long buffers respectively. This is illustrated in Figure 5 where the numerator of eqn. (2) is the sum of the late integrals and the denominator is the sum of all of the integrals. It is advantageous to define the PSD term in this way since each scintillator will have a different optimal late integration starting point. All computation is done offline. Figure 2 shows the results of this exercise.

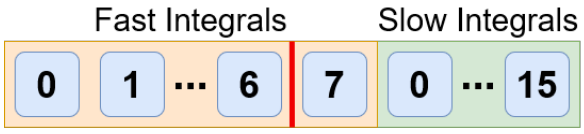

Fig. 5: Early/late integral sample boundary. To the right of the red line are late integrals; to the left are early integrals.

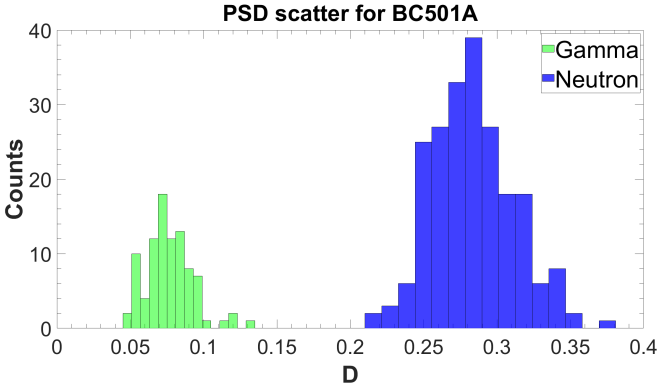

Fig. 6: Neutron/gamma distributions at 600 ± 5 keVee.

In order to quantify how well the system is discriminating between neutrons and γ-rays a common figure of merit [7] was used. The figure of merit is obtained by analyzing the distributions of D over specific energy ranges. This produces the bimodal histogram as seen in Figure 6. The figure of merit is obtained from this distribution by

$$\text{FOM} = \frac{|\mu_n - \mu_\gamma|}{\text{FWHM}_n + \text{FWHM}_\gamma} \tag{3}$$

where μ_n and μ_γ are the means of a Gaussian fit over the neutron and gamma distributions, respectively, and FWHM_n and FWHM_γ are the full width half maximums. Using this FOM a lower limit for acceptable PSD performance of FOM ≥ 1.27 can be defined, as this is the point at which the neutrons and γ-rays are separated by at least 3σ. The FOMs obtained from two distinct scintillators in the dataset are shown in Figure 7 by the solid red lines. The results are comparable to results obtained with traditional DSP systems [1].

B. Phase correction

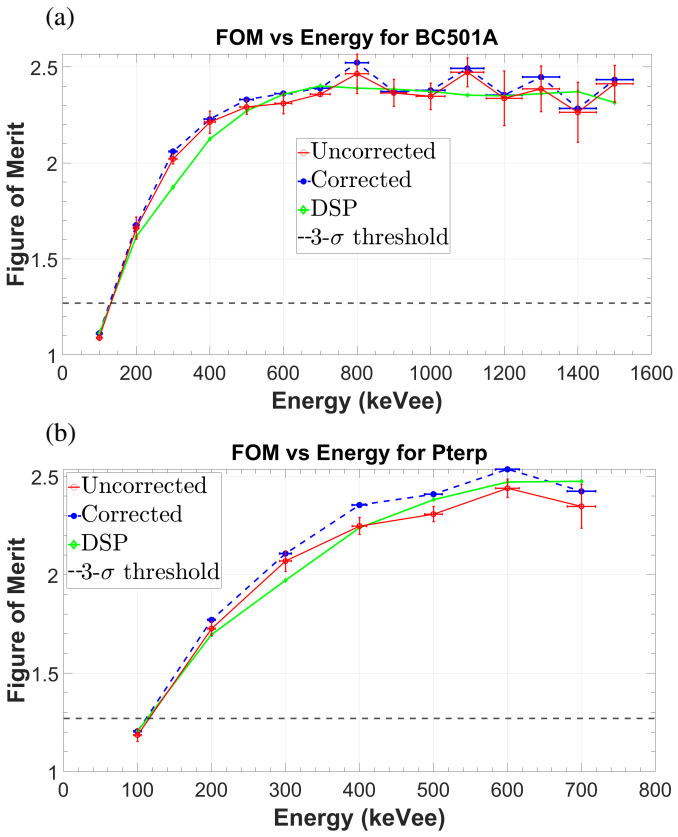

Fig. 7: Figure of merit for BC501A (a) and p-terphenyl (b) scintillators shown in red. Blue dashed line shows the FOM after phase correction is applied. The solid green line shows the FOM computed using the traditional DSP methods on the raw pulse data. Error bars on FOM are statistical, whereas the error bars on energy show the widths of the intervals chosen to determine the FOM.

One of the potential issues with the system is that the detector pulse comes asynchronously with respect to the sample clock. Since the optimal slow integration time is defined relative to the pulse peak it is possible to under integrate or over integrate into the samples on the early/late integral boundary as illustrated in Figure 8. To compensate for this

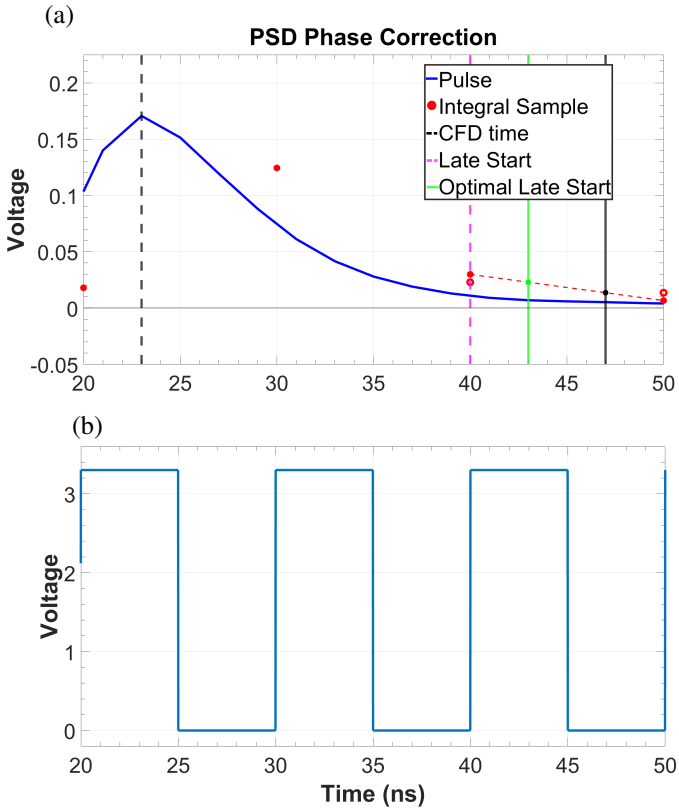

Fig. 8: Phase correction using linear interpolation (a) and sample clock (b). Open circles indicate new integral sample values after phase correction.

phase error a simple linear interpolation is performed between the two samples on the boundary of the late and early integrals. To give better time resolution, k was chosen such that a sample on either side of the optimal boundary would be in the short buffer.

Using the CFD time as a reference time the optimal late integration boundary is calculated. If this boundary does not fall on a rising edge of the sample clock the linear interpolation algorithm is used to compensate. The algorithm interpolates a line between the two samples that are separated by the boundary and then computes a new value for each of these samples by shifting them along this line by the phase difference between the CFD trigger and sample clock.

For BC501A the results were underwhelming with under 3% improvement in the FOM on average over the entire energy range. However as can be seen in Figure 7(b) the p-terphenyl scintillator is more responsive to this method with an average of 6% improvement across the entire energy range. This indicates that the ability to correct for phase error is scintillator dependent, and different algorithms may be better suited to different scintillators.

IV. Comparisons with Analog and DSP Systems

The proposed mixed-mode system has several the advantages of both analog and DSP-based systems. One of these

advantages is the ability to detect when multiple detector pulses occur very near each other in time, which is known as pile-up. In an analog system pile-up can be difficult to deal with since there are not enough sample points to determine if pile-up has occurred. In DSP this is easier since there will be double peaks in the sampled pulse. In the proposed mixed mode design pile-up can be detected similarly by observing a second peak in the tail integrals. Using this method 2.4% of the simulated pulses were able to be rejected before the FOM was generated.

In both analog and DSP systems there also exist dynamic range limitations. In the proposed design the use of two gain modes allows for increased dynamic range. In each sub-channel a programmable resistor bank is used to set the charge rate of the integrator with faster charge rates available in the high gain sub-channel. Larger amplitude pulses will saturate the integrator in the high gain mode. Since high gain and low gain sub-channels run in parallel, when saturation in the high gain sub-channel is detected, the system automatically switches to using the low gain sub channel for sampling into a long tail buffer. This allows for dynamic range enhancement without knowing a priori which gain mode is needed.

V. Conclusions and Future Work

In this paper a topology for a mixed-mode system capable of pulse-shape discrimination was proposed. The system topology was modeled using Verilog-A and simulated with real waveform data from several scintillator detectors. Results show this topology is PSD capable and offers many of the advantages of both analog and DSP-based systems. Using simple software algorithms, it is shown it is possible to improve performance by mitigating phase errors. The system analyzed is a proof of concept, and formal design optimization is in order to determine the best allocation of resources in the circuit to maximize PSD performance and detector channel counts.

Acknowledgment

This material is based upon work supported by the Department of Energy, National Nuclear Security Administration, under Award Number DE-NA0003841 and the National Science Foundation under award CNS-1763503.

References

[1] M. Sénoville, F. Delaunay, M. Pârlog, N. Achouri, and N. Orr, "Neutron-γ discrimination with organic scintillators: Intrinsic pulse shape and light yield contributions," *Nucl. Instr. and Meth. A*, vol. 971, p. 164080, 2020.

[2] C. Sosa, M. Flaska, and S. Pozzi, "Comparison of analog and digital pulse-shape-discrimination systems," *Nucl. Instr. and Meth. A*, vol. 826, pp. 72–79, 2016.

[3] R. Aryaeinejad, J. Hartwell, and D. Spencer, "Comparison between digital and analog pulse shape discrimination techniques for neutron and gamma ray separation," in *IEEE Nuclear Science Symp. Conf. Record*, vol. 1, 2005, pp. 500–504.

[4] G. Engel, N. Duggireddi, V. Vangapally, J. Elson, L. Sobotka, and R. Charity, "Multi-channel integrated circuits for the detection and measurement of ionizing radiation," *Nucl. Instr. and Meth. A*, vol. 652, no. 1, pp. 462–465, 2011.

[5] G. Engel, M. Hall, J. Proctor, J. Elson, L. Sobotka, R. Shane, and R. Charity, "Design and performance of a multi-channel, multi-sampling, PSD-enabling integrated circuit," *Nucl. Instr. and Meth. A*, vol. 612, no. 1, pp. 161–170, 2009.

[6] J.-M. Régis, M. Rudigier, J. Jolie, A. Blazhev, C. Fransen, G. Pascovici, and N. Warr, "The time-walk of analog constant fraction discriminators using very fast scintillator detectors with linear and non-linear energy response," *Nucl. Instr. and Meth. A*, vol. 684, pp. 36–45, 2012.

[7] W. G. J. Langeveld, M. J. King, J. Kwong, and D. T. Wakeford, "Pulse shape discrimination algorithms, figures of merit, and gamma-rejection for liquid and solid scintillators," *IEEE Trans. on Nuclear Science*, vol. 64, no. 7, pp. 1801–1809, 2017.